

MATHEMATICAL MODEL OF OPTIMIZATION OF THE TRANSPARENT PARTITION THICKNESS IN THE TROMBE WALL HEAT EXCHANGE SYSTEM

Ivan K. Andrianov, Elena K. Chepurnova, Sergey A. Kostikov

Institute of Machine Science and Metallurgy of the Far Eastern Branch of the Russian Academy of Sciences of the Khabarovsk Federal Research Center of the Far Eastern Branch of the Russian Academy of Sciences, Komsomolsk-na-Amure, RUSSIA

Abstract: The study is devoted to the issue of mathematical modeling of effective heat transfer in a Trombe wall, which is a structural element of passive solar heating of buildings. The problem of optimization the geometry of the transparent partition wall of the Trombe wall, partially absorbing and transmitting solar energy, is considered in the work. The air temperature in the air layer is selected as the optimization objective function. A mathematical model for optimizing the wall thickness of a transparent partition, at which the maximum air temperature in the gap is reached, is built in the work. The model was constructed using the equations of thermal balance, the Bouguer-Lambert-Beer law, and the necessary and sufficient conditions for the extremum of the objective function. The determining ratios take into account the processes of convective and radiant heat transfer. The numerical calculation method is implemented using the implicit differentiation method and the Newton iterative method. The optimal values of the wall thickness of a transparent partition, at which the maximum value of the air temperature in the wall layer of the Trombe wall is reached, as well as the corresponding temperatures of the partition and the surface of a massive wall coated with a phase transition material, are obtained based on the constructed mathematical model. The constructed graphical dependences of the air temperature in the gap on the wall thickness of the transparent partition clearly demonstrate the presence of a maximum of the objective function. The optimal values of the wall thickness of the transparent partition and the air temperature in the interlayer decrease with increasing absorption coefficient of the glass partition material according to the results of numerical experiments. The constructed mathematical model and numerical calculation method will make it possible to increase the efficiency of heat transfer in the Trombe wall by reducing heat energy losses when choosing the optimal thickness of the glass partition.

Keywords: Trombe wall, system of passive heating, solar radiation, convective heat exchange, radiant heat exchange, optimization, implicit differentiation

МАТЕМАТИЧЕСКАЯ МОДЕЛЬ ОПТИМИЗАЦИИ ТОЛЩИНЫ СТЕНКИ ПРОЗРАЧНОЙ ПЕРЕГОРОДКИ В СИСТЕМЕ ТЕПЛООБМЕНА СТЕНЫ ТРОМБА

И.К. Андрианов, С.А. Костиков, Е.К. Чепурнова

Институт машиноведения и металлургии Дальневосточного отделения Российской академии наук Федерального государственного бюджетного учреждения науки Хабаровского Федерального исследовательского центра Дальневосточного отделения Российской академии наук, г. Комсомольск-на-Амуре, РОССИЯ

Аннотация: Исследование посвящено вопросу математического моделирования эффективного теплопереноса в стене Тромба, представляющей собой конструктивный элемент пассивного солнечного отопления зданий. В работе рассматривается проблема оптимизации геометрии прозрачной перегородки стены Тромба, частично поглощающей и пропускающей солнечную энергию. В качестве целевой функции оптимизации выбрана температура воздуха в воздушной прослойке. Построена математическая модель оптимизации толщины стенки прозрачной перегородки, при которой достигается максимальная температура воздуха в зазоре. Построение модели проводилось с использованием уравнений теплового баланса, закона Бугера-Ламберта-Бера, необходимого и достаточного условий экстремума целевой функции. Определяю-

щие соотношения учитывают процессы конвективного и лучистого теплообмена. Численная методика расчета реализована с использованием метода неявного дифференцирования и итерационного метода Ньютона. На основании построенной математической модели получены оптимальные значения толщины стенки прозрачной перегородки, при которых достигается максимальное значение температуры воздуха в прослойке стены Тромба, а также соответствующие значения температур перегородки и поверхности массивной стены с покрытием из материала с фазовым переходом. Построенные графические зависимости температуры воздуха в прослойке от толщины стенки прозрачной перегородки наглядно демонстрируют наличие максимума целевой функции. Согласно результатам численных экспериментов при увеличении коэффициента поглощения материала стеклянной перегородки, оптимальные значения толщины ее стенки и температуры воздуха в прослойке уменьшаются. Построенная математическая модель и численная методика расчета позволят повысить эффективность теплопереноса в стене Тромба за счет снижения потерь тепловой энергии при выборе оптимальной толщины стеклянной перегородки.

Ключевые слова: стена Тромба, системы пассивного отопления, солнечное излучение, конвективный теплообмен, лучистый теплообмен, оптимизация, неявное дифференцирование

1. INTRODUCTION

Today, research on the use of heat exchange systems based on renewable energy sources is becoming increasingly common in civil and structural engineering. One such system is the Trombe wall, which operates by accumulating solar energy. The operating principle of this system is as follows: the flow of solar radiation, passing through a transparent partition, is absorbed by a solid wall, which is coated with a dark coating of a phase-change material. The absorbed thermal energy is then transferred to the air space between the transparent partition and the solid wall [1-3]. In practice, the Trombe wall is used as a source of passive heating in the design of residential structures.

In recent years, various approaches to optimizing the Trombe wall have become widespread, reflected primarily in foreign studies. The most comprehensive discussion of modern trends in Trombe wall optimization is provided in [4]. In addition, the main optimization issues addressed in the study of heat transfer in a Trombe wall should be noted: the choice of coatings and phase-change materials that ensure the best heat transfer in the Trombe wall [5, 6]; modeling the operating conditions of the Trombe wall to ensure optimal thermal comfort [7]; reducing energy consumption and heat losses in the Trombe wall [8, 9]; optimizing the geometry and introducing new design solutions in the Trombe wall [10, 11]; developing software to control the heat

transfer process in the Trombe wall [12, 13]. According to the conducted analysis, most of the studied Trombe wall optimization problems are solved by trying out various configurations using either numerical methods, in particular the finite element method, or with the help of full-scale experiments. A few works are devoted to mathematical modeling of heat transfer in the Trombe wall, in particular the works [3, 14]. Some issues related to improving thermal efficiency in construction, as well as the use of phase-change materials, are discussed in [15-20].

One unexplored issue remains the mathematical modeling of the optimal thickness of the transparent partition in a Trombe wall. Today, a wide variety of glass blocks, double-glazed windows are used as transparent partitions in Trombe walls, each with varying degrees of light transmittance, which affects the amount of solar energy absorbed by the transparent partition. The challenge of optimizing the thickness of the transparent partition stems from the fact that, on the one hand, it acts as a thermal barrier: the thicker the transparent partition wall, the more light it absorbs, and the higher its temperature. On the other hand, as the thickness of the transparent partition wall increases, the intensity of solar radiation transmitted through the partition and incident on the solid wall with a phase-change material coating decreases. Since one of the main functions of a Trombe wall is to heat the air in the air gap between the transparent partition and the solid wall, the development of a mathematical model for optimizing the thickness of the

transparent partition, ensuring the maximum air temperature in the air gap of the Trombe wall, is relevant.

When conducting mathematical modeling of the optimal wall thickness of a transparent partition in the heat transfer system of a Trombe wall, we will use the following assumptions:

- the boundary surfaces of the transparent partition and the solid wall are flat, the width of the air gap and the thickness of the transparent partition are constant,
- the intensity of solar radiation incident on the Trombe wall is constant over the period of time under consideration,
- the reflection of solar radiation on the outer surface of the transparent partition is negligible,
- the boundary surfaces of the transparent partition and the solid wall are isothermal in the studied region,
- the air temperature and the heat transfer coefficient on the outer surface of the transparent partition remain constant over the studied period of time,
- the air temperature field in the studied region of the air gap is uniform,
- the temperature of the outer surface of the solid wall with a coating made of a phase-change material does not exceed the melting point of the material,
- heat transfer through the solid wall with a coating made of a phase-change material is excluded.

2. METHODS

Let us consider the heat balance equations for a transparent partition, air in the air gap and a solid wall with a coating made of a phase-change material [3]:

$$Q_{gl}^+ - Q_{gl}^- = c_{gl}\rho_{gl}\delta S (T_{gl}^{(\tau)} - T_{gl}^{(0)}), \quad (1)$$

$$Q_{air}^+ - Q_{air}^- = c_{air}\rho_{air}bS (T_{air}^{(\tau)} - T_{air}^{(0)}), \quad (2)$$

$$Q_{wl}^+ - Q_{wl}^- = c_{wl}m_{wl} (T_{wl}^{(\tau)} - T_{wl}^{(0)}), \quad (3)$$

where Q_{gl}^+, Q_{gl}^- – the amounts of heat supplied to and removed from the transparent partition, Q_{air}^+, Q_{air}^- – the amounts of heat supplied to and removed from the air in the air gap, Q_{wl}^+, Q_{wl}^- – the amounts of heat supplied to and removed from the massive wall with a coating made of phase-change material, c_{gl}, c_{air}, c_{wl} – the specific heat capacities of the transparent partition, air in the duct, and phase-change material, ρ_{gl}, ρ_{air} – the densities of the transparent partition, air in the duct, m_{wl} – the mass of the phase-change material, δ – the thickness of the transparent partition, b – the width of the air duct, $T_{gl}^{(0)}, T_{air}^{(0)}, T_{wl}^{(0)}$ – the initial temperatures of the transparent partition, air in the duct, and phase-change material, $T_{gl}^{(\tau)}, T_{air}^{(\tau)}, T_{wl}^{(\tau)}$ – temperatures of the transparent partition, air in the channel, material with a phase transition after time τ .

We will describe the attenuation of the luminous flux when light radiation passes through the wall of a transparent partition based on the Bouguer-Lambert-Beer law:

$$I = I_0 e^{-\mu\delta}, \quad (4)$$

where I_0 – the intensity of the light flux incident on the transparent partition, I – the intensity of the light flux passed through the transparent partition, μ – the absorption coefficient of the medium.

Heat supply and removal (Fig. 1) is ensured by radiant and convective heat exchange, taking into account the relationship (4):

$$Q_{gl}^+ = I_0(1 - e^{-\mu\delta})S\tau + \alpha_{gl}^+ (T_{air}^{(\tau)} - T_{gl}^{(\tau)})S\tau + \varepsilon\sigma \left((T_{wl}^{(\tau)})^4 - (T_{gl}^{(\tau)})^4 \right) S\tau,$$

$$Q_{gl}^- = \varepsilon\sigma \left((T_{gl}^{(\tau)})^4 - T_{out}^4 \right) S\tau + \alpha_{gl}^- (T_{gl}^{(\tau)} - T_{out})S\tau,$$

$$Q_{air}^+ = \alpha_{wl} (T_{wl}^{(\tau)} - T_{air}^{(\tau)})S\tau,$$

$$Q_{air}^- = \alpha_{gl}^+ (T_{air}^{(\tau)} - T_{gl}^{(\tau)})S\tau,$$

$$Q_{wl}^+ = I_0 e^{-\mu\delta} S\tau,$$

$$Q_{wl}^- = \varepsilon\sigma \left((T_{wl}^{(\tau)})^4 - (T_{gl}^{(\tau)})^4 \right) S\tau + \alpha_{wl} (T_{wl}^{(\tau)} - T_{air}^{(\tau)}) S\tau,$$

where $T_{out}^{(\tau)}$ – the outside air temperature, α_{gl}^+ , α_{gl}^- – the heat transfer coefficients on the boundary

inner and outer surfaces of the transparent partition, α_{wl} – the heat transfer coefficient on the surface of a massive wall with a coating made of a phase-change material, S – the area of the surface under study, ε is the effective emissivity, σ – the Stefan-Boltzmann constant.

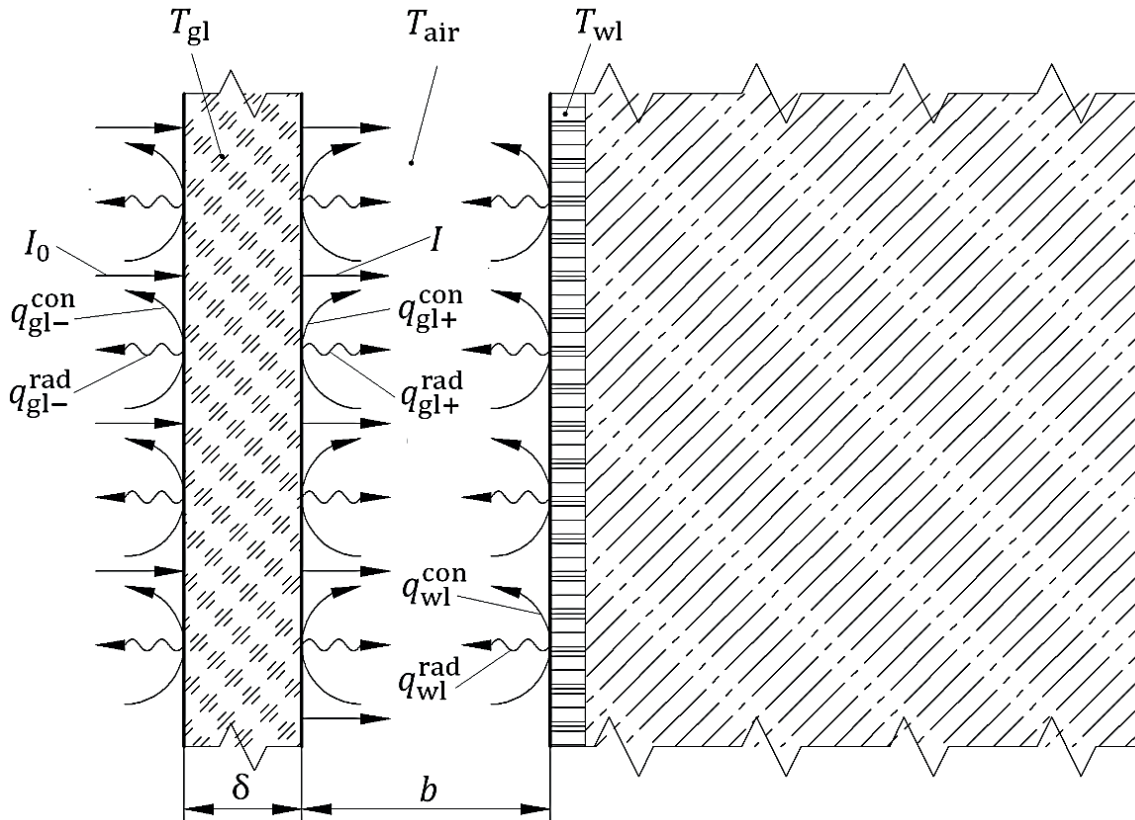


Figure 1. Diagram of the heat exchange process in the Trombe wall (q_{gl-}^{rad} , q_{gl+}^{rad} , q_{wl}^{rad} – specific radiant heat flux on the outer and inner surfaces of the transparent partition and on the surface of the massive wall; q_{gl-}^{con} , q_{gl+}^{con} , q_{wl}^{con} – specific convective heat flux on the outer and inner surfaces of the transparent partition and on the surface of the massive wall)

When constructing the optimization model, we will consider an unconstrained optimization problem. The objective function will be the air temperature in the air gap between the transparent partition and the solid wall coated with a phase-change material, and the optimization variable will be the wall thickness of the transparent partition. Thus, the mathematical formulation of the air optimization problem in the gap, taking into account heat balance equations (1) –(3) and

the Bouguer-Lambert-Beer law, will take the form:

$$T_{air}^{(\tau)} = T_{air}^{(\tau)} (\delta, T_{wl}^{(\tau)}(\delta), T_{gl}^{(\tau)}(\delta)) \rightarrow \max, \quad (5)$$

$$\Phi_1 (\delta, T_{air}^{(\tau)}(\delta), T_{wl}^{(\tau)}(\delta), T_{gl}^{(\tau)}(\delta)) = 0, \quad (6)$$

$$\Phi_2 (T_{air}^{(\tau)}(\delta), T_{wl}^{(\tau)}(\delta), T_{gl}^{(\tau)}(\delta)) = 0, \quad (7)$$

$$\Phi_3 (\delta, T_{air}^{(\tau)}(\delta), T_{wl}^{(\tau)}(\delta), T_{gl}^{(\tau)}(\delta)) = 0, \quad (8)$$

$$\begin{aligned}
 \text{where } \Phi_1 &= c_{gl}\rho_{gl}\delta\left(T_{gl}^{(\tau)} - T_{gl}^{(0)}\right) - I_0(1 - e^{-\mu\delta})\tau - \varepsilon\sigma\left(\left(T_{wl}^{(\tau)}\right)^4 - \left(T_{gl}^{(\tau)}\right)^4\right)\tau + \\
 &+ \varepsilon\sigma\left(\left(T_{gl}^{(\tau)}\right)^4 - \left(T_{out}^{(\tau)}\right)^4\right)\tau + \\
 &+ \alpha_{gl}^-\left(T_{gl}^{(\tau)} - T_{out}^{(\tau)}\right)\tau - \alpha_{gl}^+\left(T_{air}^{(\tau)} - T_{gl}^{(\tau)}\right)\tau, \\
 \Phi_2 &= c_{air}\rho_{air}b\left(T_{air}^{(\tau)} - T_{air}^{(0)}\right) - \\
 &- \alpha_{wl}\left(T_{wl}^{(\tau)} - T_{air}^{(\tau)}\right)\tau + \alpha_{gl}^+\left(T_{air}^{(\tau)} - T_{gl}^{(\tau)}\right)\tau, \\
 \Phi_3 &= c_{wl}m_{wl}\left(T_{wl}^{(\tau)} - T_{wl}^{(0)}\right) - I_0e^{-\mu\delta}S\tau + \\
 &+ \varepsilon\sigma\left(\left(T_{wl}^{(\tau)}\right)^4 - \left(T_{gl}^{(\tau)}\right)^4\right)S\tau \\
 &+ \alpha_{wl}\left(T_{wl}^{(\tau)} - T_{air}^{(\tau)}\right)S\tau.
 \end{aligned}$$

To find the optimal value for the transparent partition wall thickness, we use the necessary extremum condition: $\left.\frac{\partial T_{air}}{\partial \delta}\right|_{\delta=\delta^*} = 0$, where δ^* – the optimal value for the transparent partition wall thickness. According to the system of equations (5) – (8), the air temperature in the air gap is not explicitly expressed in terms of the wall thickness. Therefore, we use the implicit differentiation method:

$$\begin{aligned}
 \frac{d\Phi_1}{d\delta} &= \frac{\partial\Phi_1}{\partial\delta} + \frac{\partial\Phi_1}{\partial T_{air}} \frac{\partial T_{air}}{\partial\delta} + \\
 &+ \frac{\partial\Phi_1}{\partial T_{wl}} \frac{\partial T_{wl}}{\partial\delta} + \frac{\partial\Phi_1}{\partial T_{gl}} \frac{\partial T_{gl}}{\partial\delta}, \quad (9)
 \end{aligned}$$

$$\begin{aligned}
 \frac{d\Phi_2}{d\delta} &= \frac{\partial\Phi_2}{\partial\delta} + \frac{\partial\Phi_2}{\partial T_{air}} \frac{\partial T_{air}}{\partial\delta} + \\
 &+ \frac{\partial\Phi_2}{\partial T_{wl}} \frac{\partial T_{wl}}{\partial\delta} + \frac{\partial\Phi_2}{\partial T_{gl}} \frac{\partial T_{gl}}{\partial\delta}, \quad (10)
 \end{aligned}$$

$$\begin{aligned}
 \frac{d\Phi_3}{d\delta} &= \frac{\partial\Phi_3}{\partial\delta} + \frac{\partial\Phi_3}{\partial T_{air}} \frac{\partial T_{air}}{\partial\delta} + \\
 &+ \frac{\partial\Phi_3}{\partial T_{wl}} \frac{\partial T_{wl}}{\partial\delta} + \frac{\partial\Phi_3}{\partial T_{gl}} \frac{\partial T_{gl}}{\partial\delta}. \quad (11)
 \end{aligned}$$

Solving the system of equations (9) – (11) taking into account the conditions:

$$\begin{aligned}
 \left.\frac{\partial T_{air}}{\partial \delta}\right|_{\delta=\delta^*} &= 0 \text{ and } d\Phi_1/d\delta = 0, \\
 d\Phi_2/d\delta &= 0, d\Phi_3/d\delta = 0,
 \end{aligned}$$

according to equations (6) – (8), and excluding $\partial T_{wl}/\partial \delta$, $\partial T_{gl}/\partial \delta$, we move on to the equation for $\delta = \delta^*$:

$$\Phi_4\left(\delta^*, T_{air}^{(\tau)}(\delta^*), T_{wl}^{(\tau)}(\delta^*), T_{gl}^{(\tau)}(\delta^*)\right) = 0, \quad (12)$$

where

$$\begin{aligned}
 \Phi_4 &= \frac{\partial\Phi_1}{\partial\delta} - \frac{\partial\Phi_1}{\partial T_{wl}^{(\tau)}} \frac{\partial\Phi_3}{\partial\delta} / \frac{\partial\Phi_3}{\partial T_{wl}^{(\tau)}} + \\
 &+ \left(\frac{\partial\Phi_1}{\partial T_{gl}^{(\tau)}} - \frac{\partial\Phi_1}{\partial T_{wl}^{(\tau)}} \frac{\partial\Phi_3}{\partial T_{gl}^{(\tau)}} / \frac{\partial\Phi_3}{\partial T_{wl}^{(\tau)}}\right) \cdot \\
 &\cdot \left[\frac{\partial\Phi_2}{\partial T_{wl}^{(\tau)}} \frac{\partial\Phi_3}{\partial\delta} / \frac{\partial\Phi_3}{\partial T_{wl}^{(\tau)}}\right] / \left(\frac{\partial\Phi_2}{\partial T_{gl}^{(\tau)}} - \frac{\partial\Phi_2}{\partial T_{wl}^{(\tau)}} \frac{\partial\Phi_3}{\partial T_{gl}^{(\tau)}} / \frac{\partial\Phi_3}{\partial T_{wl}^{(\tau)}}\right), \\
 \partial\Phi_1/\partial\delta &= c_{gl}\rho_{gl}\left(T_{gl}^{(\tau)} - T_{gl}^{(0)}\right) - \\
 -\mu I_0 e^{-\mu\delta}\tau, \quad \partial\Phi_1/\partial T_{wl}^{(\tau)} &= -4\varepsilon\sigma\left(T_{wl}^{(\tau)}\right)^3\tau, \\
 \partial\Phi_1/\partial T_{gl}^{(\tau)} &= c_{gl}\rho_{gl}\delta + 8\varepsilon\sigma\left(T_{gl}^{(\tau)}\right)^3\tau + \\
 + (\alpha_{gl}^- + \alpha_{gl}^+)\tau, \quad \partial\Phi_2/\partial T_{wl}^{(\tau)} &= -\alpha_{wl}\tau, \\
 \partial\Phi_2/\partial T_{gl}^{(\tau)} &= -\alpha_{gl}^+\tau, \\
 \partial\Phi_3/\partial T_{gl}^{(\tau)} &= -4\varepsilon\sigma\left(T_{gl}^{(\tau)}\right)^3S\tau, \\
 \partial\Phi_3/\partial T_{wl}^{(\tau)} &= c_{wl}m_{wl} + 4\varepsilon\sigma\left(T_{wl}^{(\tau)}\right)^3S\tau + \\
 + \alpha_{wl}S\tau, \quad \partial\Phi_3/\partial\delta &= \mu I_0 e^{-\mu\delta}S\tau.
 \end{aligned}$$

Thus, the optimization problem is reduced to solving the system of equations (6) – (8), (12) for $\delta = \delta^*$. We introduce the vector of unknown parameters: $\mathbf{x} = \{\delta, T_{air}^{(\tau)}, T_{wl}^{(\tau)}, T_{gl}^{(\tau)}\}$. To calculate the system of nonlinear equations, we use Newton's iterative method, then the linearized system of equations (6) – (8), (12) will take the form:

$$\begin{aligned}
 \sum_{j=1}^4 \frac{\partial\Phi_i(\mathbf{x}^k)}{\partial x_j} \Delta x_j^{k+1} + \Phi_i(\mathbf{x}^k) &= 0, i = \overline{1,4}, \\
 x_j^{k+1} &= \Delta x_j^{k+1} + x_j^k, \quad (13)
 \end{aligned}$$

where k – the iteration number.

The condition for the termination of the iterative process can be represented as: $\max_{1 \leq j \leq 4} |x_j^{k+1} - x_j^k| \leq \Delta \varepsilon$, where $\Delta \varepsilon$ – the specified accuracy of the numerical calculation.

The solution to the system of linear equations (13) will be the values: δ^* , $T_{\text{air}}^{(\tau)}(\delta^*)$, $T_{\text{wl}}^{(\tau)}(\delta^*)$, $T_{\text{gl}}^{(\tau)}(\delta^*)$, at which the air temperature in the air gap reaches the optimal value:

$$\begin{aligned} \max T_{\text{air}}^{(\tau)}(\delta, T_{\text{wl}}^{(\tau)}(\delta), T_{\text{gl}}^{(\tau)}(\delta)) &= \\ &= T_{\text{air}}^{(\tau)}(\delta^*, T_{\text{wl}}^{(\tau)}(\delta^*), T_{\text{gl}}^{(\tau)}(\delta^*)). \end{aligned}$$

In order to estimate the obtained optimal value to the maximum, we will use the sufficient condition for the extremum $\partial^2 T_{\text{air}} / \partial \delta^2 |_{\delta=\delta^*} < 0$. By solving the system of equations (9) – (11), we obtain an equation for finding $\partial T_{\text{air}} / \partial \delta$ in implicit form:

$$\Phi_5(\delta, T_{\text{air}}^{(\tau)}(\delta), T_{\text{wl}}^{(\tau)}(\delta), T_{\text{gl}}^{(\tau)}(\delta)) = 0, \quad (14)$$

where

$$\begin{aligned} \Phi_5 &= \frac{\partial \Phi_1}{\partial \delta} + \frac{\partial \Phi_1}{\partial T_{\text{air}}^{(\tau)}} \frac{\partial T_{\text{air}}^{(\tau)}}{\partial \delta} - \\ &- \frac{\partial \Phi_1}{\partial T_{\text{wl}}^{(\tau)}} \left(\frac{\partial \Phi_3}{\partial \delta} + \frac{\partial \Phi_3}{\partial T_{\text{air}}^{(\tau)}} \frac{\partial T_{\text{air}}^{(\tau)}}{\partial \delta} \right) / \frac{\partial \Phi_3}{\partial T_{\text{wl}}^{(\tau)}} + \\ &+ \left(\frac{\partial \Phi_1}{\partial T_{\text{gl}}^{(\tau)}} - \frac{\partial \Phi_1}{\partial T_{\text{wl}}^{(\tau)}} \frac{\partial \Phi_3}{\partial T_{\text{gl}}^{(\tau)}} / \frac{\partial \Phi_3}{\partial T_{\text{wl}}^{(\tau)}} \right) \cdot \\ &\cdot \left[\frac{\partial \Phi_2}{\partial T_{\text{wl}}^{(\tau)}} \left(\frac{\partial \Phi_3}{\partial \delta} + \frac{\partial \Phi_3}{\partial T_{\text{air}}^{(\tau)}} \frac{\partial T_{\text{air}}^{(\tau)}}{\partial \delta} \right) / \frac{\partial \Phi_3}{\partial T_{\text{wl}}^{(\tau)}} - \right. \\ &\left. - \frac{\partial \Phi_2}{\partial T_{\text{air}}^{(\tau)}} \frac{\partial T_{\text{air}}^{(\tau)}}{\partial \delta} \right] / \left(\frac{\partial \Phi_2}{\partial T_{\text{gl}}^{(\tau)}} - \frac{\partial \Phi_2}{\partial T_{\text{wl}}^{(\tau)}} \frac{\partial \Phi_3}{\partial T_{\text{gl}}^{(\tau)}} / \frac{\partial \Phi_3}{\partial T_{\text{wl}}^{(\tau)}} \right), \\ \frac{\partial \Phi_1}{\partial T_{\text{air}}^{(\tau)}} &= -\alpha_{\text{gl}}^+ \tau, \quad \frac{\partial \Phi_3}{\partial T_{\text{air}}^{(\tau)}} = -\alpha_{\text{wl}} \tau, \\ \frac{\partial \Phi_2}{\partial T_{\text{air}}^{(\tau)}} &= c_{\text{air}} \rho_{\text{air}} b + (\alpha_{\text{wl}} + \alpha_{\text{gl}}^+) \tau. \end{aligned}$$

We introduce the notation $T_{\text{air}}^{(\tau)'} = \partial T_{\text{air}}^{(\tau)} / \partial \delta$. To check the sufficient condition for the extremum to be maximal, we use the implicit differentiation method. Then, taking into account that $d\Phi_5 / d\delta = 0$, we obtain an equation for calculating $\partial T_{\text{air}}^{(\tau)'} / \partial \delta$:

$$\begin{aligned} \frac{\partial \Phi_5}{\partial \delta} + \frac{\partial \Phi_5}{\partial T_{\text{air}}^{(\tau)'}} \frac{\partial T_{\text{air}}^{(\tau)'}}{\partial \delta} + \frac{\partial \Phi_5}{\partial T_{\text{wl}}^{(\tau)}} \frac{\partial T_{\text{wl}}^{(\tau)}}{\partial \delta} + \\ + \frac{\partial \Phi_5}{\partial T_{\text{gl}}^{(\tau)}} \frac{\partial T_{\text{gl}}^{(\tau)}}{\partial \delta} = 0, \end{aligned} \quad (15)$$

where

$$\begin{aligned} \frac{\partial T_{\text{wl}}^{(\tau)}}{\partial \delta} &= - \left(\frac{\partial \Phi_3}{\partial \delta} + \frac{\partial \Phi_3}{\partial T_{\text{air}}^{(\tau)}} \frac{\partial T_{\text{air}}^{(\tau)}}{\partial \delta} + \right. \\ &\left. + \frac{\partial \Phi_3}{\partial T_{\text{gl}}^{(\tau)}} \frac{\partial T_{\text{gl}}^{(\tau)}}{\partial \delta} \right) / \frac{\partial \Phi_3}{\partial T_{\text{wl}}^{(\tau)'}} \\ \frac{\partial T_{\text{gl}}^{(\tau)}}{\partial \delta} &= \left[\frac{\partial \Phi_2}{\partial T_{\text{wl}}^{(\tau)}} \left(\frac{\partial \Phi_3}{\partial \delta} + \frac{\partial \Phi_3}{\partial T_{\text{air}}^{(\tau)}} \frac{\partial T_{\text{air}}^{(\tau)}}{\partial \delta} \right) / \frac{\partial \Phi_3}{\partial T_{\text{wl}}^{(\tau)}} - \right. \\ &\left. - \frac{\partial \Phi_2}{\partial T_{\text{air}}^{(\tau)}} \frac{\partial T_{\text{air}}^{(\tau)}}{\partial \delta} \right] / \\ &/ \left(\frac{\partial \Phi_2}{\partial T_{\text{gl}}^{(\tau)}} - \frac{\partial \Phi_2}{\partial T_{\text{wl}}^{(\tau)}} \frac{\partial \Phi_3}{\partial T_{\text{gl}}^{(\tau)}} / \frac{\partial \Phi_3}{\partial T_{\text{wl}}^{(\tau)}} \right) \end{aligned}$$

The solution to equation (15) for $\delta = \delta^*$ is $\partial^2 T_{\text{air}} / \partial \delta^2 |_{\delta=\delta^*}$. Due to nonlinearity, the numerical solution to equation (15) can be found using Newton's method, similar to the system of equations (13).

To establish the dependence of the temperature change: $T_{\text{air}}^{(\tau)}$, $T_{\text{wl}}^{(\tau)}$, $T_{\text{gl}}^{(\tau)}$ with a change in δ , we consider the numerical solution of the system of equations (6) - (8) with a vector of unknown parameters $\mathbf{x} = \{T_{\text{air}}^{(\tau)}, T_{\text{wl}}^{(\tau)}, T_{\text{gl}}^{(\tau)}\}$ for a given set of values of the thickness of the transparent partition $\boldsymbol{\delta} = \{\delta_l\}$, $l = \overline{1, n}$. Applying Newton's method for the numerical solution of the system

of equations (6) - (8), we obtain the following iterative scheme for a fixed value of the partition thickness $\delta = \delta_l, l = \overline{1, n}$:

$$\sum_{j=1}^4 \frac{\partial \Phi_i(\mathbf{x}^k, \delta_l)}{\partial x_j} \Delta x_j^{k+1} + \Phi_i(\mathbf{x}^k, \delta_l) = 0, \quad (16)$$

$$x_j^{k+1} = \Delta x_j^{k+1} + x_j^k, \quad i = \overline{1, 3}, j = \overline{1, 4}, l = \overline{1, n}.$$

The condition for the termination of the iterative process: $\max_{1 \leq j \leq 3} |x_j^{k+1} - x_j^k| \leq \Delta \varepsilon$. The initial approximations of the sought temperatures in the iterative processes (13) and (16) will be determined by the given values at the initial moment of time: $T_{\text{air}}^{(0)}, T_{\text{wl}}^{(0)}, T_{\text{gl}}^{(0)}$.

3. RESULTS

Based on the constructed mathematical models, we will carry out a numerical calculation using the mathematical package Mathcad 15.0 with the following input data: $\mu = 1,05, I_0 = 350 \text{ W/m}^2, \tau = 300 \text{ s}, \sigma = 5,67 \cdot 10^{-8} \text{ W/(m}^2 \cdot \text{K}^4), \varepsilon = 0,3, \alpha_{\text{gl}}^+ = 8 \text{ W/(m}^2 \cdot \text{K}), \alpha_{\text{gl}}^- = 23 \text{ W/(m}^2 \cdot \text{K}), \alpha_{\text{wl}} = 8 \text{ W/(m}^2 \cdot \text{K}), c_{\text{wl}} = 3000 \text{ J/(kg} \cdot \text{K}), c_{\text{gl}} = 840 \text{ J/(kg} \cdot \text{K}), c_{\text{air}} =$

$1005 \text{ J/(kg} \cdot \text{K}), S = 1 \text{ m}^2, b = 0,1 \text{ m}, m_{\text{wl}} = 7,2 \text{ kg}, \rho_{\text{air}} = 1,5 \text{ kg/m}^3, \rho_{\text{gl}} = 2500 \text{ kg/m}^3, T_{\text{wl}}^{(0)} = 293 \text{ K}, T_{\text{gl}}^{(0)} = 293 \text{ K}, T_{\text{air}}^{(0)} = 293 \text{ K}, T_{\text{out}}^{(0)} = 288 \text{ K}, \Delta \varepsilon = 0,01.$

We will consider a glass partition as a transparent partition. We will conduct a series of calculations for various values of the glass absorption coefficient: $\mu_1 = \mu, \mu_2 = 5\mu, \mu_3 = 10\mu, \mu_4 = 20\mu$. We will take the initial approximation of the optimal glass wall thickness in the iterative process (13) as $\delta^0 = 1 \text{ mm}$.

According to the numerical solution of the optimization problem (5) – (8) for different values of the absorption coefficient of the glass, the following optimal values were obtained, presented in Table 1.

To estimate the temperature changes of the glass partition, the air in the air gap, and the surface of a solid wall coated with a phase-change material for various values of a given set of glass partition thicknesses: $\delta = \{2, 4, \dots, 12, 15, 25, 50, \dots, 100\} \text{ mm}$, numerical solutions of the system of equations (6)–(8) were obtained. Graphical dependences of the change in the desired temperatures on the glass partition thickness are presented in Fig. 2.

Table 1. Results of calculating the optimal parameters in problem (5) – (8)

Absorption coefficient, $\mu_i(\mu), i = \overline{1, 4}$	Optimal parameters			
	$\delta^*, \text{ mm}$	$T_{\text{air}}^*, \text{ }^\circ\text{C}$	$T_{\text{wl}}^*, \text{ }^\circ\text{C}$	$T_{\text{gl}}^*, \text{ }^\circ\text{C}$
$\mu_1 = \mu$	53,89	21,96	24,23	19,80
$\mu_2 = 5\mu$	23,04	21,76	23,96	19,68
$\mu_2 = 10\mu$	15,87	21,67	23,78	19,66
$\mu_2 = 20\mu$	10,93	21,58	23,55	19,69

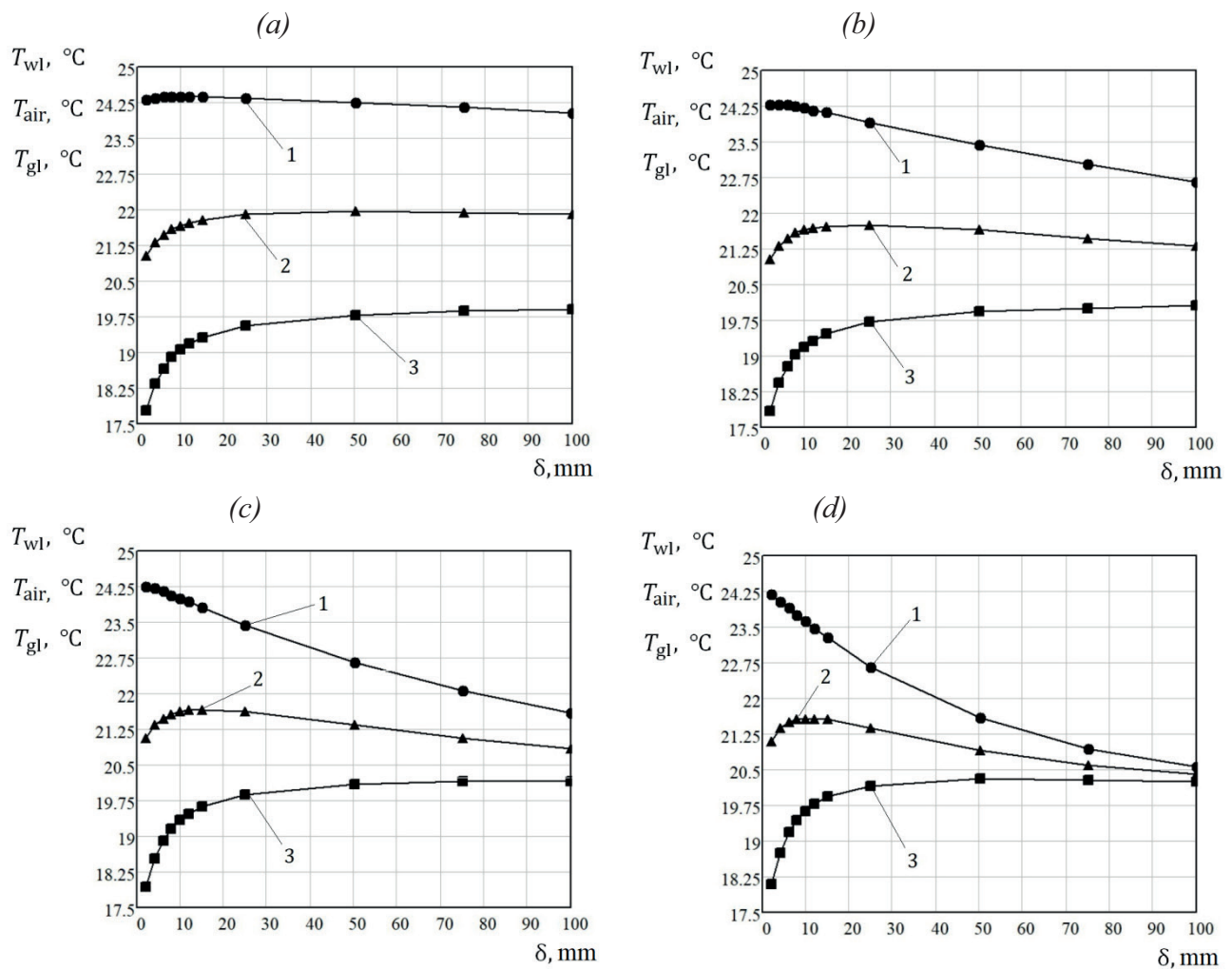


Figure 2. Dependence of the temperatures of a solid wall (1), air in the air gap (2), glass partition (3) on the thickness of the glass partition with absorption coefficients: $\mu_1 = \mu$ (a), $\mu_2 = 5\mu$ (b), $\mu_3 = 10\mu$ (c), $\mu_4 = 20\mu$ (d)

4. DISCUSSION

According to the results presented in Table 1, optimal values for the glass partition thickness were obtained for achieving the maximum air temperature in the Trombe wall air gap, as well as the corresponding temperatures of the glass partition and the surface of the solid wall coated with a phase-change material. As the glass partition's absorption coefficient increases, the optimal thickness and the maximum air temperature in the Trombe wall air gap decrease.

The graphical dependencies presented in Figure 2 clearly demonstrate the presence of a maximum on the curve of the air temperature in the Trombe

wall air gap as a function of the glass partition thickness. Moreover, the optimal values in the graphs in Figure 2 correspond to the values obtained in Table 1, confirming the accuracy of the numerical calculations performed according to the constructed mathematical model. Based on the results presented in Figure 2, it can be concluded that as the thickness of the transparent partition increases, the air temperature in the air gap initially increases, then reaches a maximum value, and then decreases; With an increase in the absorption coefficient of the glass partition, all other things being equal, the maximum point on the curve of the dependence for the air tempera-

ture in the air gap shifts “to the left”, i.e. the optimal values of the thickness of the transparent partition are achieved at smaller values.

5. CONCLUSION

This paper develops a mathematical model for calculating the optimal wall thickness of a transparent partition in a Trombe wall, achieving the maximum air temperature in the air gap between a solid wall coated with a phase-change material and the transparent partition. The mathematical model takes into account heat balance conditions for convective and radiative heat transfer, as well as the Bouguer-Lambert-Beer law. The numerical solution to the optimization problem was constructed using the implicit differentiation method and Newton's iterative method. Numerical experiments yielded optimal temperatures for the glass partition, the air in the air gap, and the surface of the solid wall coated with a phase-change material. These temperatures were also plotted as a function of the wall thickness of the transparent partition in the Trombe wall. According to the obtained results, as the absorption coefficient of the glass partition used as a transparent partition in the Trombe wall increases, the optimal wall thickness and the maximum air temperature in the air gap decrease. It should be noted that in practice, a transparent partition can be a single-chamber glass unit with an effective thickness of 25 mm. A transparent partition can also be a glass block with an effective thickness ranging from 75 mm to 100 mm.

ACKNOWLEDGEMENTS

The research was funded by the Russian Science Foundation grant №25-29-01248, <https://rscf.ru/project/25-29-01248/>.

REFERENCES

1. **Bryzgalin V.V., Soloviev A.K.** (2018). Use of passive solar heating systems as an element of a passive house. *Vestnik MGSU*, 13(4), 472–481. <https://doi.org/10.22227/1997-0935.2018.4.472-481>
2. **Bi Z.** (2024). Use of Trombe walls to improve energy efficiency in Harbin, Shenyang and Changchun during heating periods. *Ekonomika Stroitel'stva*, (12), 588–591.
3. **Kostikov S.A., Grinkrug M.S., Gordin S.A., Yiqiang J.** (2023). Numerical study of thermal characteristics of a new Trombe wall design with glass blocks for cold climatic conditions. *Teploenergetika*, (12), 90–100. <https://doi.org/10.56304/S004036362312007X>
4. **Xiao Yu., Yang Q., Fei F., et al.** (2024). Review of Trombe wall technology: Trends in optimization. *Renewable and Sustainable Energy Reviews*, 200, 114503. <https://doi.org/10.1016/j.rser.2024.114503>
5. **Zhou Ya., Zhu J., Zhang Yu., et al.** (2024). Structure and regional optimization of a phase change material Trombe wall system. *Energy*, 305, 132273. <https://doi.org/10.1016/j.energy.2024.132273>
6. **Martínez A., Alonso C., Martín-Con-suegra F., et al.** (2021). Experimental analysis of a prototype for a thermochromic Trombe wall. *Building Research and Information*, 49(7), 777–794. <https://doi.org/10.1080/09613218.2021.1905502>
7. **Bensafi M., Bayram M., Osra O., et al.** (2023). Optimization of thermal comfort in buildings via analysis of a Trombe wall for enhanced energy efficiency. *Thermal Science*, 27(4 Part B), 3423–3432. <https://doi.org/10.2298/tsci2304423b>
8. **Zhu Na., Deng R., Hu P., et al.** (2021). Coupling optimization study of key influencing factors on PCM Trombe wall for year-round thermal management. *Energy*, 236, 121470. <https://doi.org/10.1016/j.energy.2021.121470>
9. **Samiev K. A., Halimov A. S., Fayziev Sh. Sh.** (2022). Multiobjective optimization of integration of the Trombe wall in buildings using a full factorial experiment. *Applied*

- Solar Energy*, 58(1), 127–136. <https://doi.org/10.3103/s0003701x22010169>
10. **Bevilacqua P., Bruno R., Gallo S., & Szyszka J.** (2024). A validated multi-physic model for the optimization of an innovative Trombe Wall for winter use. *Journal of Building Engineering*, 86, 108915. <https://doi.org/10.1016/j.jobe.2024.108915>
 11. **Zamora B., Kaiser A. S.** (2009). Thermal and dynamic optimization of the convective flow in Trombe Wall shaped channels by numerical investigation. *Heat and Mass Transfer*, 45(11), 1393–1407. <https://doi.org/10.1007/s00231-009-0509-6>
 12. **Hashemi S. H., Dinmohammad M., Hashemi S. A.** (2021). Optimization of Trombe wall system parameters using TWSim software. *Modeling Earth Systems and Environment*, 7(2), 917–924. <https://doi.org/10.1007/s40808-020-00929-0>
 13. **Kostikov S. A.** (2021). Optimization of design solutions for Trombe wall. In *Aktual'nye problemy informatsionno-telekommunikatsionnykh tekhnologii i matematicheskogo modelirovaniya v sovremennoi nauke i promyshlennosti: Materialy I Mezhdunarodnoi nauchno-prakticheskoi konferentsii molodykh uchenykh* (pp. 158–161). Komsomolsk-on-Amur: Komsomolsk-on-Amur State University. <https://doi.org/10.17084/978-5-7765-1488-3-2021-158>
 14. **Kostikov S. A.** (2021). Prediction of thermal load of a combined building heating system based on mathematical modeling. In S. I. Sukhorukov, A. S. Gudim, & N. N. Lyubushkina (Eds.), *Proizvodstvennye tekhnologii budushchego: ot sozdaniya k vnedreniyu: Materialy IV Mezhdunarodnoi nauchno-prakticheskoi konferentsii* (pp. 276–280). Komsomolsk-on-Amur: Komsomolsk-on-Amur State University.
 15. **Tusnina V. M.** (2023). Numerical analysis of thermal efficiency of external walls with heat-conducting inclusions. *International Journal for Computational Civil and Structural Engineering*, 19(1), 155–167. <https://doi.org/10.22337/2587-9618-2023-19-1-155-167>
 16. **Fedosov S. V., Anisimova N. K., Shchepochkina Yu. A., Shishkov Yu. V.** (2011). Non-stationary heat transfer in two-layer unlimited plate at combined boundary conditions of the second and fourth types. *International Journal for Computational Civil and Structural Engineering*, 7(1), 33–38.
 17. **Nevskii S. A., Kormyshev V. E., Simonov Y. N., Konovalov S. V.** (2020). Simulation of phase transformations in high carbon pearlite steel at various cooling rates. *CIS Iron and Steel Review*, 20, 55–60. <https://doi.org/10.17580/cisirs.2020.02.12>
 18. **Zhu N., Li S., Hu P., Lei F., Deng R.** (2019). Numerical investigations on performance of phase change material Trombe wall in building. *Energy*, 187(C).
 19. **Andrianov I. K.** (2025). On the formulation of the problem of optimizing the thickness of the transparent partition wall in the Trombe wall heat exchange system. In *Prikladnaya matematika i fundamental'naya informatika: Materialy XV Mezhdunarodnoi molodezhnoi nauchno-prakticheskoi konferentsii s elementami nauchnoi shkoly* (pp. 10–11). Omsk: Omsk State Technical University.
 20. **Zhao J., Ma X., Zhang Q.** (2025). Buildings' thermal performance and energy efficiency for sustainable construction. *Buildings*, 15(18), 3410

СПИСОК ЛИТЕРАТУРЫ

1. **Брызгалин В. В., Соловьев А. К.** Использование пассивных систем солнечного отопления как элемента пассивного дома. Вестник МГСУ, 2018, Т. 13, № 4(115), С. 472–481. DOI: 10.22227/1997-0935.2018.4.472-481.
2. **Би Ж.** Использование Стен Тромба для повышения энергоэффективности в го-

- роде Харбин, Шэньян и Чанчунь в периоды отопления. Экономика строительства, 2024, № 12, С. 588–591.
3. **Костиков С. А., Гринкруг М. С., Гордин С. А., Yiqiang J.** Численное исследование тепловых характеристик стены Тромба новой конструкции со стеклоблоком для холодных климатических условий. Теплоэнергетика, 2023, № 12, С. 90–100. DOI: 10.56304/S004036362312007X.
 4. **Xiao Yu., Yang Q., Fei F. et al.** Review of Trombe wall technology: Trends in optimization. Renewable and Sustainable Energy Reviews, 2024, Vol. 200, P. 114503. DOI: 10.1016/j.rser.2024.114503.
 5. **Zhou Ya., Zhu J., Zhang Yu. et al.** Structure and regional optimization of a phase change material Trombe wall system. Energy, 2024, Vol. 305, P. 132273. DOI: 10.1016/j.energy.2024.132273.
 6. **Martínez A., Alonso C., Martín-Consegra F. et al.** Experimental analysis of a prototype for a thermochromic Trombe wall. Building Research and Information, 2021, Vol. 49, No. 7, P. 777–794. DOI: 10.1080/09613218.2021.1905502.
 7. **Bensafi M., Bayram M., Osra O. et al.** Optimization of thermal comfort in buildings via analysis of a Trombe wall for enhanced energy efficiency. Thermal Science, 2023, Vol. 27, No. 4 Part B, P. 3423–3432. DOI: 10.2298/tsci2304423b.
 8. **Zhu Na, Deng R., Hu P. et al.** Coupling optimization study of key influencing factors on PCM Trombe wall for year-round thermal management. Energy, 2021, Vol. 236, P. 121470. DOI: 10.1016/j.energy.2021.121470.
 9. **Samiev K. A., Halimov A. S., Fayziev Sh. Sh.** Multiobjective optimization of integration of the Trombe wall in buildings using a full factorial experiment. Applied Solar Energy, 2022, Vol. 58, No. 1, P. 127–136. DOI: 10.3103/s0003701x22010169.
 10. **Bevilacqua P., Bruno R., Gallo S., Szyszka J.** A validated multi-physic model for the optimization of an innovative Trombe Wall for winter use. Journal of Building Engineering, 2024, Vol. 86, P. 108915. DOI: 10.1016/j.jobe.2024.108915.
 11. **Zamora B., Kaiser A. S.** Thermal and dynamic optimization of the convective flow in Trombe Wall shaped channels by numerical investigation. Heat and Mass Transfer, 2009, Vol. 45, No. 11, P. 1393–1407. DOI: 10.1007/s00231-009-0509-6.
 12. **Hashemi S. H., Dinmohammad M., Hashemi S. A.** Optimization of Trombe wall system parameters using TWsim software. Modeling Earth Systems and Environment, 2021, Vol. 7, No. 2, P. 917–924. DOI: 10.1007/s40808-020-00929-0.
 13. **Костиков С. А.** Оптимизация конструктивных решений для стены Тромба. В кн.: Актуальные проблемы информационно-телекоммуникационных технологий и математического моделирования в современной науке и промышленности: Материалы I Международной научно-практической конференции молодых учёных, Комсомольск-на-Амуре, 20–25 марта 2021 года. Комсомольск-на-Амуре: Комсомольский-на-Амуре государственный университет, 2021, С. 158–161. DOI: 10.17084/978-5-7765-1488-3-2021-158.
 14. **Костиков С. А.** Прогнозирование тепловой нагрузки комбинированной системы теплоснабжения здания на основе математического моделирования. В кн.: Производственные технологии будущего: от создания к внедрению: Материалы IV Международной научно-практической конференции, Комсомольск-на-Амуре, 16–26 февраля 2021 года / Редколлегия: С. И. Сухоруков (отв. ред.), А. С. Гудим, Н. Н. Любушкина. Комсомольск-на-Амуре: Комсомольский-на-Амуре государственный университет, 2021, С. 276–280.
 15. **Tusnina V. M.** Numerical analysis of thermal efficiency of external walls with heat-conducting inclusions. International Journal for Computational Civil and Structural Engineering, 2023, Vol. 19, No. 1, P. 155–167. DOI: 10.22337/2587-9618-2023-19-1-155-167.

16. **Федосов С. В., Анисимова Н. К., Щепочкина Ю. А., Шишков Ю. В.** Нестационарный теплообмен в двухслойной неограниченной пластине при комбинированных граничных условиях второго и четвертого типов. *International Journal for Computational Civil and Structural Engineering*, 2011, Vol. 7, No. 1, P. 33–38.
17. **Nevskii S. A., Kormyshev V. E., Simonov Y. N., Konovalov S. V.** Simulation of phase transformations in high carbon pearlite steel at various cooling rates. *CIS Iron and Steel Review*, 2020, Vol. 20, P. 55–60. DOI: 10.17580/cisr.2020.02.12.
18. **Zhu N., Li S., Hu P., Lei F., Deng R.** Numerical investigations on performance of phase change material Trombe wall in building. *Energy*, 2019, Vol. 187(C).
19. **Андрианов И. К.** К постановке задачи об оптимизации толщины стенки прозрачной перегородки в системе теплообмена стены Тромба. В кн.: *Прикладная математика и фундаментальная информатика: Материалы XV Международной молодежной научно-практической конференции с элементами научной школы, Омск, 19–24 мая 2025 года*. Омск: Омский государственный технический университет, 2025, С. 10–11.
20. **Zhao J., Ma X., Zhang Q.** Buildings' thermal performance and energy efficiency for sustainable construction. *Buildings*, 2025, Vol. 15, No. 18, P. 3410. DOI: 10.3390/buildings15183410.

Ivan K. Andrianov, Ph.D. in engineering sciences, associate professor, senior researcher, Institute of Machine Science and Metallurgy, Far Eastern Branch of the Russian Academy of Sciences (IMiM FEB RAS – a separate subdivision of the Khabarovsk Federal Research Center, FEB RAS), 1 Metallurgov St., Komsomolsk-on-Amur, Khabarovsk Krai, 681005, Russia, e-mail: ivan_andrianov_90@mail.ru,

Иван Константинович Андрианов, кандидат технических наук, доцент, старший научный сотрудник, Институт машиноведения и металлургии Дальневосточного отделения Российской академии наук Федерального государственного бюджетного учреждения науки Хабаровского Федерального исследовательского центра Дальневосточного отделения Российской академии наук (ИМиМ ДВО РАН - обособленное подразделение ХФИЦ ДВО РАН), дом 1, ул. Металлургов, Хабаровский край, г. Комсомольск-на-Амуре, 681005, Россия, ivan_andrianov_90@mail.ru.

Elena K. Chepurnova, junior researcher, Institute of Machine Science and Metallurgy, Far Eastern Branch of the Russian Academy of Sciences (IMiM FEB RAS – a separate subdivision of the Khabarovsk Federal Research Center, FEB RAS), 1 Metallurgov St., Komsomolsk-on-Amur, Khabarovsk Krai, 681005, Russia, e-mail: el.chep@bk.ru.

Елена Константиновна Чепурнова, младший научный сотрудник, Институт машиноведения и металлургии Дальневосточного отделения Российской академии наук Федерального государственного бюджетного учреждения науки Хабаровского Федерального исследовательского центра Дальневосточного отделения Российской академии наук (ИМиМ ДВО РАН - обособленное подразделение ХФИЦ ДВО РАН), дом 1, ул. Металлургов, Хабаровский край, г. Комсомольск-на-Амуре, 681005, Россия, el.chep@bk.ru.

Sergey A. Kostikov, junior researcher, Institute of Machine Science and Metallurgy, Far Eastern Branch of the Russian Academy of Sciences (IMiM FEB RAS – a separate subdivision of the Khabarovsk Federal Research Center, FEB RAS), 1 Metallurgov St., Komsomolsk-on-Amur, Khabarovsk Krai, 681005, Russia, e-mail: 300gloof@mail.ru.

Сергей Александрович Костиков, младший научный сотрудник, Институт машиноведения и металлургии Дальневосточного отделения Российской академии наук Федерального государственного бюджетного учреждения науки Хабаровского Федерального исследовательского центра Дальневосточного отделения Российской академии наук (ИМиМ ДВО РАН - обособленное подразделение ХФИЦ ДВО РАН), дом 1, ул. Металлургов, Хабаровский край, г. Комсомольск-на-Амуре, 681005, Россия, 300gloof@mail.ru.